Dalton Transactions

PAPER

View Article Online
View Journal | View Issue

Cite this: *Dalton Trans.*, 2014, **43**, 16310

1,3,5-Triferrocenyl-2,4,6-tris(ethynylferrocenyl)-benzene – a new member of the family of multiferrocenyl-functionalized cyclic systems†‡

Ulrike Pfaff, Grzegorz Filipczyk, Alexander Hildebrandt, Marcus Korb and Heinrich Lang*

The consecutive synthesis of 1,3,5-triferrocenyl-2,4,6-tris(ethynylferrocenyl)benzene (**6c**) is described using 1,3,5-Cl_3-2,4,6-I_3-C_6 (**2**) as starting compound. Subsequent Sonogashira *C,C* cross-coupling of **2** with FcC≡CH (**3**) in the molar ratio of 1 : 4 afforded solely 1,3,5-Cl_3-2,4,6-$(FcC{\equiv}C)_3$-C_6 (**4c**) (Fc = Fe(η^5-C_5H_4)(η^5-C_5H_5)). However, when **2** is reacted with **3** in a 1 : 3 ratio a mixture of 1,3,5-Cl_3-2-(FcC≡C)-4,6-I_2-C_6 (**4a**) and 1,3,5-Cl_3-2,4-$(FcC{\equiv}C)_2$-6-I-C_6 (**4b**) is obtained. Negishi *C,C* cross-coupling of **4c** with FcZnCl (**5**) in the presence of catalytic amounts of $[Pd(CH_2C(CH_3)_2P(^tC_4H_9)_2)(\mu\text{-}Cl)]_2$ gave 1,3-Cl_2-5-Fc-2,4,6-$(FcC{\equiv}C)_3$-C_6 (**6a**), 1-Cl-3,5-Fc_2-2,4,6-$(FcC{\equiv}C)_3$-C_6 (**6b**) and 1,3,5-Fc_3-2,4,6-$(FcC{\equiv}C)_3$-C_6 (**6c**) of which **6b** is the main product. Column chromatography allowed the separation of these organometallic species. The structures of **4a**,**b** and **6a** in the solid state were determined by single crystal X-ray diffractometry showing a π–π interacting dimer (**4b**) and a complex π–π pattern for **6a**. The electrochemical properties of **4a–c** and **6a–c** were studied by cyclic voltammetry (=CV) and square wave voltammetry (=SWV). It was found that the FcC≡C-substituted benzenes **4a–c** show only one reversible redox event, indicating a simultaneous oxidation of all ferrocenyl units, whereby **4c** is most difficult to oxidise (**4a**, $E°'_1$ = 190, ΔE_p = 71; **4b**, $E°'_1$ = 195, ΔE_p = 59; **4c**, $E°'_1$ = 390, ΔE_p = 59 mV). In case of **4c**, the oxidation states $\mathbf{4c}^{n+}$ (n = 2, 3) are destabilised by the partial negative charge of the electronegative chlorine atoms, which compensates the repulsive electrostatic Fc^+–Fc^+ interactions with attractive electrostatic Fc^+–$Cl^{\delta-}$ interactions. When ferrocenyl units are directly attached to the benzene C_6 core, organometallic **6a** shows three, **6b** five and **6c** six separated reversible waves highlighting that the Fc units can separately be oxidised. UV-Vis/NIR spectroscopy allowed to determine IVCT absorptions (=Inter Valence Charge Transfer) for $\mathbf{6c}^{n+}$ (n = 1, 2) (n = 1: ν_{max} = 7860 cm^{-1}, ε_{max} = 405 L mol^{-1} cm^{-1}, $\Delta\nu_{1/2}$ = 7070 cm^{-1}; n = 2: ν_{max} = 9070 cm^{-1}, ε_{max} = 620 L mol^{-1} cm^{-1}, $\Delta\nu_{1/2}$ = 8010 cm^{-1}) classifying these mixed-valent species as weakly coupled class II systems according to Robin and Day, while for **6a,b** only LMCT transitions (=ligand to metal charge transfer) could be detected.

Received 29th July 2014,
Accepted 22nd August 2014

DOI: 10.1039/c4dt02307b

www.rsc.org/dalton

Introduction

Multiferrocenyl-functionalized aromatics and heteroaromatics are fascinating molecules. Besides their uncommon molecular structures, such sterically crowded compounds possess, for example, interesting electronic properties.[1] Hence, they can be considered as model systems to study intramolecular electron transfer through π-conjugated carbon-rich organic linking units *via* the mixed-valence states derived from these multi-metallic compounds. In this respect, the ferrocenyl group is beneficial since the [Fe(II)/Fe(III)] redox couple shows an excellent electrochemical reversibility and high thermal stability.[2] The degree of electronic communication among the appropriate metal centers has mostly been explored by electrochemical studies such as cyclic voltammetry (=CV), square wave voltammetry (=SWV) and spectroelectrochemistry (*e.g.*, *in situ* UV-Vis/NIR spectroscopy). Other relevant applications for reversible multi-step redox systems include their use in the field of catalysis,[3] in biological studies[4] or as novel molecular electro-active materials.[5]

Super-crowded ferrocenyl-based organometallic compounds are moreover remarkable species because the expected steric

Technische Universität Chemnitz, Faculty of Natural Sciences, Institute of Chemistry, Inorganic Chemistry, D-09107 Chemnitz, Germany. E-mail: heinrich.lang@chemie.tu-chemnitz.de; Fax: +49 (0)371-531-21219; Tel: +49 (0)371-531-21210

† Dedicated to Prof. Dr Gerhard Roewer on the occasion of his 75th birthday.

‡ Electronic supplementary information (ESI) available: ORTEP diagram of **4b** and **6a**, deconvolution of the square wave voltammogram of **6a**, cyclic and square wave voltammograms of **8** and **9** and UV-Vis/NIR spectra of compounds **6a,b** and **9**. Crystallographic data of **4a,b** and **6a** are also available. CCDC 986632 (**4a**), 986631 (**4b**) and 1009947 (**6a**). For ESI and crystallographic data in CIF or other electronic format see DOI: 10.1039/c4dt02307b

encumbrance may hinder chemical conjugation between the aromatic core and the ferrocenyl substituents. Representatives of this class of compounds are, for example, ferrocenyl-end-grafted dendrimers[6,7] in which the intramolecular distance between the ferrocenyls is enlarged by various units such as ethynyl,[6a–c] ethynyl benzene,[6d–e] and ethynyl thiophene[1f] or amidoamine-based dendrimers.[7] Further examples of multi-ferrocenyl organometallic compounds are benzenes,[6b,c,8,9] 5-membered heterocycles[10,11] or even cobalt[12] and manganese[13] half-sandwich species with up to six terminal ferrocenyl or ethynyl ferrocenyl entities, *i.e.* $(FcC{\equiv}C)_6C_6$, Fc_6C_6, 2,3,4,5-Fc_4-^cC_4E (E = O, S, NPh, NMe), $Co(\eta^4$-$Fc_4C_4)(\eta^5$-$C_5H_5)$, and Mn-$(\eta^5$-$Fc_5C_5)(CO)_3$. Electrochemical studies revealed that for the respective super-crowded ferrocenyl thiophene significant electrostatic interaction among the four ferrocenyl groups occurs as oxidation progresses. The spectroelectrochemical results showed several UV-Vis and NIR peaks appearing or disappearing between 280 and 3000 nm as this compound is stepwisely oxidised to ultimately generate $[2,3,4,5$-Fc_4-$^cC_4S]^{4+}$. For the respective pyrrole compounds electronic interaction between the ferrocenyl/ferrocenium units is evidenced by *in situ* UV-Vis/NIR spectroscopy.[10b] In contrast, Vollhardt's hexaferrocenyl benzene[9] and Astruc's hexa-ethynylferrocenyl benzene[6b,c] show three separated redox events.

We here enrich this family of perferrocenylated benzenes and describe for the first time the synthesis of multiferrocenyl-substituted benzenes featuring alternating ferrocenyl and ethynyl ferrocenyl functionalities, which represent a combination of the structural motifs of Vollhardt's[9] and Astruc's[6b,c] benzenes. The physical and chemical properties of 1,3,5-Cl_3-2-$(FcC{\equiv}C)$-4,6-I_2-C_6, 1,3,5-Cl_3-2,4-$(FcC{\equiv}C)_2$-6-I-C_6, 1,3,5-Cl_3-2,4,6-$(FcC{\equiv}C)_3$-C_6, 1,3-Cl_2-5-Fc-2,4,6-$(FcC{\equiv}C)_3$-C_6, 1-Cl-3,5-Fc_2-2,4,6-$(FcC{\equiv}C)_3$-C_6 and 1,3,5-Fc_3-2,4,6-$(FcC{\equiv}C)_3$-C_6 (Fc = $Fe(\eta^5$-$C_5H_4)(\eta^5$-$C_5H_5)$) as well as their electrochemical properties will be highlighted.

Results and discussion

Synthesis and characterisation

1,3,5-Trichloro-2,4,6-triiodo-benzene (**2**),[14] which is accessible by an electrophilic aromatic substitution,[15] was utilised as starting compound for the preparation of 1,3,5-Cl_3-2,4,6-$(FcC{\equiv}C)_3$-C_6 (**4c**) in a Sonogashira *C*,*C* cross-coupling reaction[16] (Scheme 1). It appeared that four equivalents of **3** is imperative to the success of the reaction, since with a 1 : 3 stoichiometry of **2** and **3** only the mono- and di-substituted species 1,3,5-Cl_3-2-$(FcC{\equiv}C)$-4,6-I_2-C_6 (**4a**) and 1,3,5-Cl_3-2,4-$(FcC{\equiv}C)_2$-6-I-C_6 (**4b**), respectively, are formed (Scheme 1). Furthermore, the concentration of the palladium catalyst $[PdCl_2(PPh_3)_2]$ in the Sonogashira *C*,*C* cross-coupling plays a crucial role. For the synthesis of **4c**, 1 mol% of the catalyst is required to obtain virtually quantitative yield of **4c** (Experimental section), while for the synthesis of **4a** and **4b** 0.5 mol% of the palladium catalyst is adequate. The separation of **4a** from **4b** was realised by column chromatography.

The introduction of the ferrocenyl substituents in **4c** to give 1,3,5-Fc_3-2,4,6-$(FcC{\equiv}C)_3$-C_6 (**6c**) was realized by the synthetic methodology shown in Scheme 2. The best results were obtained, when 9 eq. of FcZnCl (**5**) as ferrocenyl source were reacted with **4c** under typical Negishi *C*,*C* cross-coupling conditions[17] using $[Pd(CH_2C(CH_3)_2P(^tC_4H_9)_2)(\mu$-$Cl)]_2$ (0.25 mol%) as catalyst (Scheme 2, Experimental section). After appropriate work-up, compounds **6a–c**, in which alternating Fc and FcC≡C units are attached to the benzene core, were isolated in the ratio of 1 : 11.2 : 3.6 (= **6a** : **6b** : **6c**) (Scheme 2).

The Fc and FcC≡C multi-substituted benzenes **4a–c** and **6a–c** (Schemes 1 and 2) were obtained as red (**4b**, **6b**) or orange (**4a**,**c** and **6a**,**c**) solids, which dissolve in almost all common organic solvents, including toluene, dichloromethane and tetrahydrofuran. They are stable towards air and moisture in the solid state and in solution.

For comparison (see Spectroelectrochemistry part) 1-FcC≡C-2-FcC_6H_4 (**9**) has been synthesized starting from 1-Br-2-I-C_6H_4 (**7**).[18] When **7** was reacted with FcC≡CH (**3**), then 1-bromo-2-ethynylferrocenyl benzene (**8**) was formed, which on treatment with FcZnCl (**5**) under typical Negishi *C*,*C* cross-coupling conditions gave **9**.[18]

Organometallics **4a–c** and **6a–c** have been identified by elemental analysis, NMR (^1H, $^{13}C\{^1H\}$) and IR spectroscopy as well as high resolution ESI-TOF mass spectrometry (Experimental section). In addition, they were analysed electrochemically

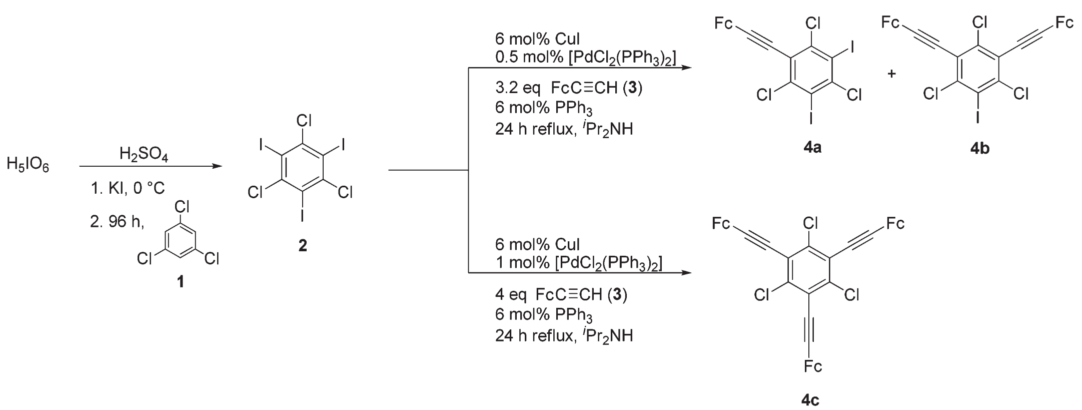

Scheme 1 Synthesis of **2**[14] and **4a–c**.

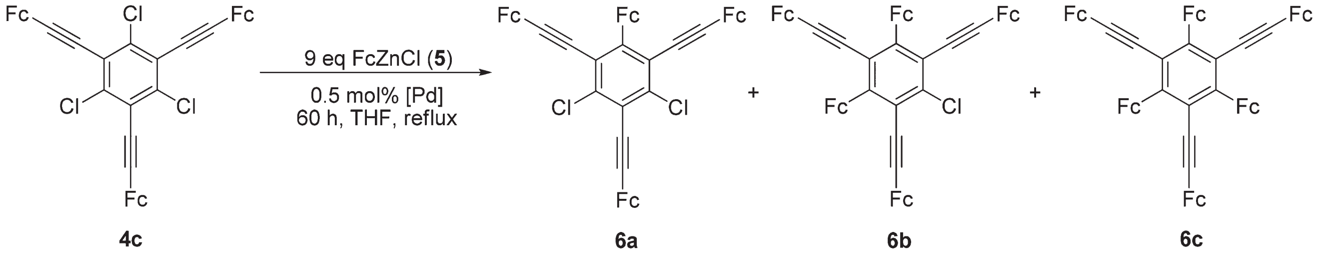

Scheme 2 Synthesis of **6a–c** from **4c** and **5** ([Pd] = [Pd($CH_2C(CH_3)_2P(^tC_4H_9)_2$)(μ-Cl)]$_2$).

using cyclic voltammetry and square wave voltammetry. Spectroelectrochemistry measurements were carried out to prove if intramolecular electron transfer occurs in the mixed-valent species using *in situ* UV-Vis/NIR spectroscopy.

The ^1H and $^{13}C\{^1H\}$ NMR spectroscopic properties of **4a–c** and **6a–c** correlate with their formulations as Fc and FcC≡C multi-functionalised benzenes showing the respective signal patterns for the Fc, C≡C and C_6 core building blocks. Most distinctive for the formation of these molecules is the appearance of the expected AA′XX′ signal pattern[19] for the C_5H_4 units (J_{HH} = 1.9 Hz) and the singlet for the C_5H_5 moieties (Experimental section). Further characteristic in the $^{13}C\{^1H\}$ NMR spectra of all complexes are the signals for the ethynyl units, which resonate at *ca.* 65 ppm (C≡*C*–C_6) and *ca.* 100 ppm (C≡*C*–Fc), respectively (Experimental section). 2D experiments such as COSY, HSQC and HMBC were applied to assign the carbon signals in **4a–c** and **6a–c** unequivocally. Most characteristic in the IR spectrum of all newly synthesised compounds is the appearance of one sharp C≡C stretching vibration between 2200 and 2220 cm^{-1}, specific for this distinctive unit.[20]

The formation of **4a–c** and **6a–c** was additionally evidenced from ESI-TOF mass spectrometric investigations. All organometallic compounds show the molecular ion peak $[M]^+$ (Experimental section). Moreover, comparison of the measured isotope patterns (Cl, I) of **4a–c** and **6a,b** with the calculated ones confirm the elemental composition and charge state.

Furthermore, single crystal X-ray diffraction studies have been carried out to determine the molecular structures of **4a** (Fig. 1), **4b** (Fig. 2) and **6a** (Fig. 3) in the solid state. Suitable single crystals of **4a,b** and **6a** could be obtained either by crystallisation of **4a** and **6a** from dichloromethane solutions, or by slow diffusion of *n*-hexane into a dichloromethane solution containing **4b** at ambient temperature (Experimental section). Important bond distances (Å), bond angles (°) and torsion angles (°) are summarised in the captions of Fig. 1–3. For crystal and structure refinement data see ESI.‡ Compound **4a** crystallises in the triclinic space group $P\bar{1}$, **4b** in the monoclinic space group $C2/c$ and **6a** in the orthorhombic space group *Pccn*.

The asymmetric unit for **4a** contains one molecule, whereas half of a dimer of **4b** is characteristic for the unit cell. In the case of **6a**, two molecules describe the asymmetric unit. The carbon–carbon bond lengths of the benzene cores of **4a,b** and **6a** in (average 1.394 Å) (Fig. 1–3) are in agreement with the

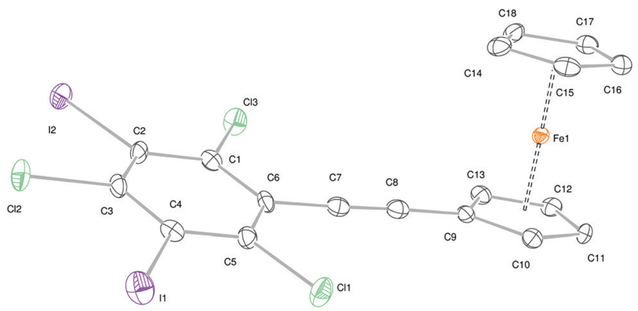

Fig. 1 ORTEP diagram (50% probability level) of the molecular structure of **4a** with the atom numbering scheme. Hydrogen atoms are omitted for clarity. Selected bond distances (Å), angles (°) and torsion angles (°): Fe–D1 = 1.6483(5), Fe–D2 = 1.6539(4), C1–C2 = 1.393(4), C2–C3 = 1.391(4), C3–C4 = 1.393(4), C4–C5 = 1.391(4), C5–C6 = 1.397(4), C1–C6 = 1.399(4), C6–C7 = 1.430(4), C7–C8 = 1.196(4), C8–C9 = 1.423(4); D1–Fe1–D2 = 179.01(3), C8–C7–C6 = 177.5(3), C7–C8–C9 = 178.3(3), C8–C9–C10 = 125.7(3), C8–C9–C13 = 126.7(3); Cl3–C1–C6–C7 = 1.6(4), Cl1–C5–C6–C7 = −0.7(4), C7–C8–C9–C10 = −72(12), C7–C8–C9–C13 = 110(12), I1–C4–C5–Cl1 = 0.5(4), Cl3–C1–C2–I2 = 3.1(4), (D1 denotes the centroid of C_5H_4, while D2 denotes the centroid of C_5H_5).

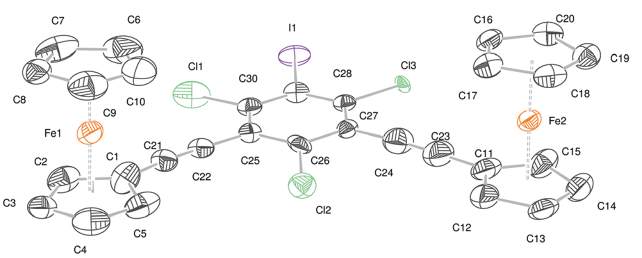

Fig. 2 ORTEP diagram (50% probability level) of the molecular structure of **4b** with the atom numbering scheme. Hydrogen atoms are omitted for clarity. Selected bond distances (Å), angles (°) and torsion angles (°): Fe1–D1 = 1.6491(15), Fe1–D2 = 1.6538(15), Fe2–D3 = 1.6479(14), Fe2–D4 = 1.6538(14), C1–C21 = 1.39(2), C21–C22 = 1.20(2), C22–C25 = 1.413(17), C11–C23 = 1.403(18), C23–C24 = 1.208(19), C24–C27 = 1.472(14); D1–Fe1–D2 = 178.40(11), D3–Fe2–D4 = 178.97(10), C1–C21–C22 = 173.3(19), C21–C22–C25 = 167.3(18), C11–C23–C24 = 179.3(18), C23–C24–C27 = 172.9(15) (D1, D3 denote the centroid of C_5H_4, while D2, D4 denote the centroid of C_5H_5).

distances found in unsubstituted benzene (1.39 Å).[21] The *C,C* distances of the ethynyl units agree with C≡C bond lengths of this type of building blocks (1.20 Å).[21]

The orientation of the cyclopentadienyl rings of the *syn*-oriented ferrocenyls to the six membered C_6 cycle is almost

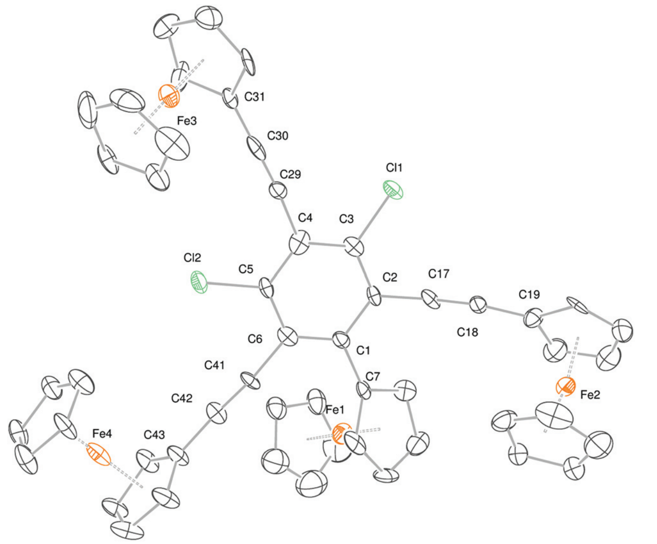

Fig. 3 ORTEP diagram (50% probability level) of the molecular structure of **6a** with the atom numbering scheme. Hydrogen atoms are omitted for clarity. Selected bond distances (Å), angles (°) and torsion angles (°): Fe1–D1 = 1.623(2), Fe1–D2 = 1.645(2), Fe2–D3 = 1.663(2), Fe2–D4 = 1.642(2), Fe3–D5 = 1.661(2), Fe3–D6 = 1.649(2), Fe4–D7 = 1.643(3), Fe4–D8 = 1.651(3), C1–C7 = 1.514(16), C6–C41 = 1.459(14), C41–C42 = 1.18(2), C42–C43 = 1.45(2), C4–C29 = 1.415(16), C29–C30 = 1.23(2), C30–C31 = 1.42(2), C2–C17 = 1.440(16), C17–C18 = 1.20(2), C18–C19 = 1.43(2), C3–Cl1 = 1.720(7), C5–Cl2 = 1.724(7); D1–Fe1–D2 = 175.69(18), D3–Fe2–D4 = 178.07(16), D5–Fe3–D6 = 178.28(17), D7–Fe4–D8 = 179.23(16), C18–C17–C2 = 171.7(14), C30–C29–C4 = 174.1(14), C42–C41–C6 = 173.8(16), C7–C1–C6 = 121.1(7), C7–C1–C2 = 118.8(7); C7–C1–C2–C17 = −13.1(11), C7–C1–C6–C41 = 2.4(11), Cl1–C3–C4–C29 = −2.5(9), C29–C4–C5–Cl2 = −1.9(9), C19–C18–C17–C2 = 94.36, C43–C42–C41–C6 = −156.17, C31–C30–C29–C4 = −82.58, (D1, D3, D5, D7 denote the centroid of C_5H_4, while D2, D4, D6, D8 denote the centroid of C_5H_5).

coplanar in molecule **4b** (3.6(10), 3.5(10)°), however, it somewhat deviates from planarity in **4a** (14.6(2)°). All ferrocenyls in **4a,b** and **6a** possess an eclipsed conformation (**4a**, −0.8(2)°; **4b**, −1.4(12), 1.1(9)°; **6a**, 8.5(10), 9.0(11), 2.6(11), 1.8(12)°). The more sterically demanding FcC≡C and Fc groups are bonded to the benzene core, the lower is the coplanarity of the ferrocenyls with the C_6 unit in **6a**. However, for all iron-centroid distances in **4a,b** and **6a** as well as for all torsion angles, no significant differences occur. Reasons for the orientation of the ferrocenyls in **6a** are the T-shaped π–π interactions between two ferrocenyls including intra-molecular (Fig. 4; 4.784(11) Å) as well as inter-molecular ones (Fig. 4; 4.981(13) Å). Furthermore, π–π interactions between the C_5H_5 moieties with the benzene core (Fig. SI1‡) could be found.

Compound **4b** can best be transcribed by the symmetry operation $-x$, $1 - y$, $-z$, which results in a rectangular shaped dimer (Fig. SI3‡) with parallel displaced π–π interactions between both C_6 cycles of 3.615(13) Å.[22] Furthermore, **4b** is strongly disordered over two positions (0.6 : 0.4) in which the ferrocenes of the disordered part correspond to the corners of the rectangle formed by the initial dimer. However, the C_6 core is rotated by 45 ° providing interaction with a third ferrocenyl corner (Fig. SI2 and SI3, ESI‡).

Electrochemistry

The redox properties of **4a–c** and **6a–c** have been determined by cyclic voltammetry (=CV) and square-wave voltammetry (=SWV) (Fig. 5). Dichloromethane solutions containing the respective analyte (1.0 mmol L^{-1}) and $[^nBu_4N][B(C_6F_5)_4]$ (0.1 mol L^{-1})[10,11,23,24] as supporting electrolyte were used for the measurements. The CV studies have been performed at a

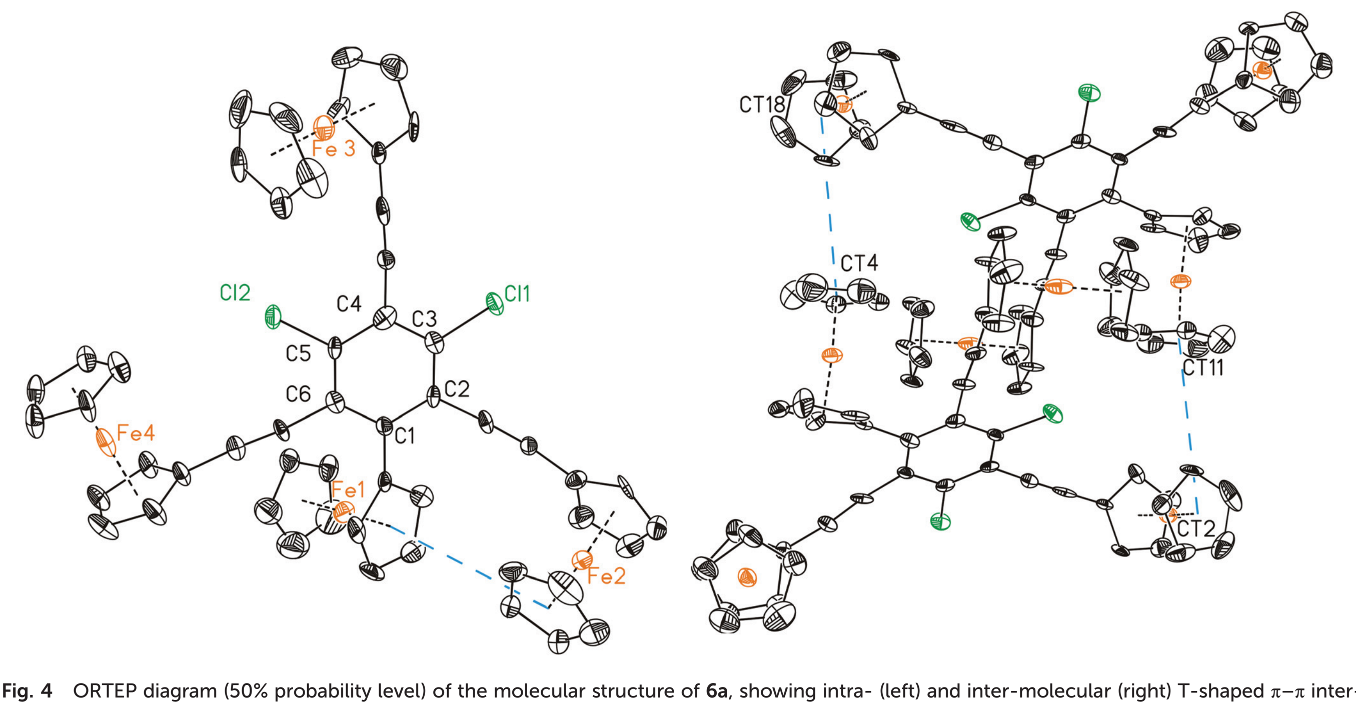

Fig. 4 ORTEP diagram (50% probability level) of the molecular structure of **6a**, showing intra- (left) and inter-molecular (right) T-shaped π–π interactions between the ferrocenyls. Hydrogen atoms are omitted for clarity. Orange: iron; green: chlorine; blue: distances between two centroids. (Left): 4.784(11) Å; (right): 4.981(13) Å.

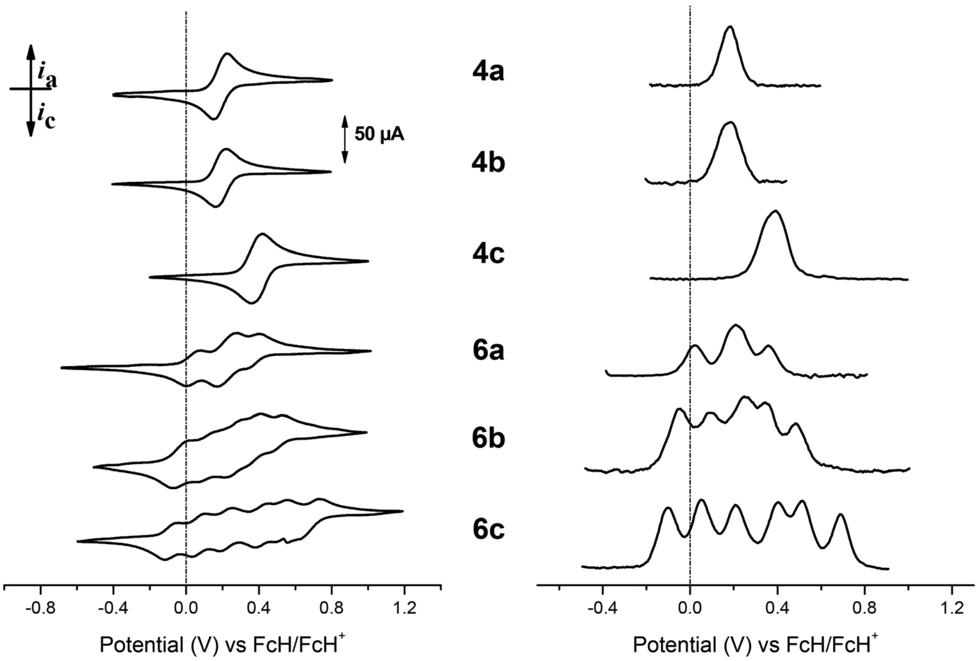

Fig. 5 Voltammograms of dichloromethane solutions containing 1.0 mmol L^{-1} of **4a–c** and **6a–c** at 25 °C. Supporting electrolyte $[^nBu_4N][B(C_6F_5)_4]$ (0.1 mol L^{-1}). Left: Cyclic voltammograms (scan rate: 100 mV s^{-1}). Right: Square-wave voltammograms (step-height: 25 mV; pulse-width: 5 s; amplitude: 5 mV).

Table 1 Cyclic voltammetry data (potentials *vs.* FcH/FcH$^+$), scan rate 100 mV s^{-1} at a glassy carbon electrode of 1.0 mmol L^{-1} solutions of the analytes in dry dichloromethane containing 0.1 mol L^{-1} of $[^nBu_4N][B(C_6F_5)_4]$ as supporting electrolyte at 25 °C. All potentials are given in [mV]

Compd	$E^{\circ\prime}_1$ [a] (ΔE_p)[b]	$E^{\circ\prime}_2$ [a] (ΔE_p)[b]	$E^{\circ\prime}_3$ [a] (ΔE_p)[b]	$E^{\circ\prime}_4$ [a] (ΔE_p)[b]	$E^{\circ\prime}_5$ [a] (ΔE_p)[b]	$E^{\circ\prime}_6$ [a] (ΔE_p)[b]	$\Delta E^{\circ\prime}$ [c]
4a	190 (71)	—	—	—	—	—	—
4b	195 (59)	—	—	—	—	—	—
4c	390 (59)	—	—	—	—	—	—
6a	40 (74)	225 (108)	360 (84)	—	—	—	185/68[d]/135
6b[e]	−50	90	250	335	485	—	140/160/85/150
6c	−80 (75)	70 (68)	220 (69)	420 (65)	530 (63)	660 (147)	150/150/200/110/130

[a] $E^{\circ\prime}$ = formal potential. [b] ΔE_p = difference between oxidation and reduction potential. [c] $\Delta E^{\circ\prime}$ = potential difference between the redox processes. [d] Potential difference between the two redox processes determined by the application of the Richardson and Taube method.[31] When using the deconvolution of the redox separation of the oxidation potentials in SWV (Fig. SI4), $\Delta E^{\circ\prime}$ = 60 mV. [e] Values determined using Square Wave Voltammetry.

scan rate of 100 mV s^{-1} and the results are summarised in Fig. 5. The appropriate potential values are given in Table 1. All redox potentials are referenced to the FcH/FcH$^+$ redox couple ($E^{\circ\prime}$ = 0 mV, FcH = Fe(η^5-C_5H_5)$_2$).[25]

From Fig. 5 it can be seen that the cyclic and square wave voltammograms of **4a–c** show only one reversible redox event irrespective of the number of FcC≡C units present, evincing the simultaneous oxidation of the Fc groups. Furthermore, it is found that an increasing number of redox-active Fc groups at the benzene core results in a shift of the $E^{\circ\prime}_1$ values to higher potentials (**4a**, $E^{\circ\prime}_1$ = 190 mV; **4b**, $E^{\circ\prime}_1$ = 195 mV; **4c**, $E^{\circ\prime}_1$ = 390 mV) (Table 1). This indicates that the more FcC≡C moieties are present, the more difficult is the oxidation of the Fe(II) centres, which is in agreement with the electron withdrawing character of the ferrocenyl ethynyl building blocks. In contrast to **4c**, 1,3,5-tris(ethynylferrocenyl) benzene (dichloromethane, $[^nBu_4N][B(3,5\text{-}C_6H_3(CF_3)_2)_4]$ as supporting electrolyte)[6b] possesses three well-separated reversible redox events with redox splittings of $\Delta E^{\circ\prime}_1 \approx 200$ mV and $\Delta E^{\circ\prime}_2 \approx 170$ mV.[6b] Geiger has shown that $[^nBu_4N][B(3,5\text{-}(CF_3)_2\text{-}(C_6H_3)_4]$ and $[^nBu_4N][B(C_6F_5)_4]$ possess quite similar ion pairing capabilities in dichloromethane and both these fluorinated borates act as very weak coordinating counter ions, thus it is expected that the appropriate $\Delta E^{\circ\prime}$ values are similar for both electrolytes.[23] Against this background the different redox behaviour of **4c** and 1,3,5-tris(ethynylferrocenyl) benzene is surprising. On the one hand it could be shown that the electronic communication between the terminal ferrocenyl units is suppressed, when electron poor aromatics are used as bridging systems.[1c,10b,26] On the other hand, the electron withdrawing effect of the chlorine atom leads to a partially negative charge, which enables attractive interactions with the neighbouring Fc$^+$C≡C units,

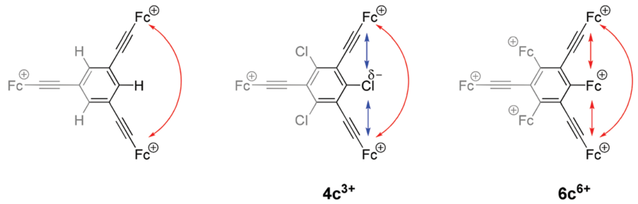

Fig. 6 Repulsive (red) and attractive (blue) electrostatic interactions within 1,3,5-tris(ethynylferrocenyl) benzene, $4c^{3+}$ and $6c^{6+}$.

compensating the repulsive electrostatic destabilisation (Fig. 6). Thus, the thermodynamic stability of mixed-valent oxidation states $\mathbf{4c}^{n+}$ (n = 1, 2) is reduced and no redox splitting could be observed. The importance of electrostatic effects on the $\Delta E^{\circ\prime}$ values especially in case of weakly coupled systems has recently been pointed out by Winter, who strongly emphasizes that $\Delta E^{\circ\prime}$ is not a sufficient measure for the electron delocalisation within mixed-valent species.[27] However, attempts to accurately model such electrostatic interactions and their effect on $\Delta E^{\circ\prime}$ may in future help for a better understanding of the electrochemical properties of mixed-valent systems.[28]

When the chlorine substituents of **4c** were stepwisely replaced with ferrocenyl units in **6a–c**, a more resolved redox behaviour with a separate oxidation of the individual ferrocenyls could be observed. A comparison of the formal oxidation potentials of ferrocenyl benzene ($E^{\circ\prime}$ = 40 mV)[29] and ethynylferrocenyl benzene ($E^{\circ\prime}$ = 115 mV)[30] allows to estimate that the ferrocenyls are oxidised prior to the FcC≡C units in **6a–c**. The oxidation potential of the 1st Fc oxidation decreases from **6a** ($E^{\circ\prime}$ = 40 mV) to **6c** ($E^{\circ\prime}$ = −80 mV) as the electron withdrawing chlorine substituents are replaced by electron-rich ferrocenyl termini. The redox splitting between the directly bonded ferrocenyl groups for **6c** ($\Delta E^{\circ\prime}_1 = \Delta E^{\circ\prime}_2$ = 150 mV) resembles those of triferrocenyl benzene ($\Delta E^{\circ\prime}_1$ = 140 mV; $\Delta E^{\circ\prime}_2$ = 145 mV). In contrast to **4c**, the ethynylferrocenyl units of **6c** are oxidised separately. For $\mathbf{6c}^{3+}$ the directly bonded Fc units are oxidised to ferrocenium termini which possess an equal or ever stronger electron withdrawing character as the chlorine substituents in **4c**, nevertheless, those groups are positively charged and therefore, add further repulsive electrostatic interactions in **6c** (Fig. 6).

Noteworthy is the high ΔE_p value of 108 mV for the second redox wave of **6a**, suggesting that two individual reversible one-electron processes take place in a close potential range. Hence, the square wave voltammogram gives an integrated peak area of 1 : 2 : 1, which verifies the presence of two closely spaced one-electron processes (Fig. 5). Deconvolution of the SWV of **6a** using four Gaussian-shaped functions resulted in $\Delta E^{\circ\prime}_2$ = 60 mV (ESI‡ Fig. SI4). The calculation of the signal width at half of the maximum current[31] to estimate the redox separation gave a similar value of $\Delta E^{\circ\prime}_2$ = 68 mV. This clearly confirms that the second oxidation process consists of two superimposed redox waves.

It was found that the reduction process of the sixth redox wave of **6c** shows a somewhat sharper current peak and hence suggests the precipitation of $\mathbf{6c}^{6+}$ on the surface of the working electrode, which is not unusual for highly charged ions.[4,24e]

Due to the use of different electrolytes in the electrochemical measurements a comparison with related work is difficult. Vollhart's hexaferrocenyl benzene gave only three redox processes consistent of a one ($E^{\circ\prime}_1$ = −163 mV), a two ($E^{\circ\prime}_2$ = −32 mV) and a three ($E^{\circ\prime}_3$ = 222 mV) electron process (dichloromethane, $[^n\mathrm{Bu_4N}][\mathrm{PF_6}]$ as supporting electrolyte).[9]

However, the use of the classical $[\mathrm{PF_6}]^-$ counter ion compensates most of the electrostatic repulsion by ion-pairing with the analyte. Hence, it is expected that the use of a weakly coordinating anion (= WCA, *i.e.* $[^n\mathrm{Bu_4N}][\mathrm{B(C_6F_5)_4}]$) would probably enable the separate oxidation of all six ferrocenyl units. In the case of hexakis(ethynylferrocenyl)benzene ($E^{\circ\prime}_1$ = −50 mV, $E^{\circ\prime}_2$ = 170 mV, $E^{\circ\prime}_3$ = 360 mV; dichloromethane, $[^n\mathrm{Bu_4N}][\mathrm{B(3,5\text{-}(CF_3)_2\text{-}(C_6H_3)_4}]$ as supporting electrolyte)[6b,c] even the use of WCA electrolytes only resulted in the observation of three reversible redox waves. The combination of both structural motifs, however, led to a well-separated redox behaviour as the ferrocenium units in-between the $\mathrm{Fc^+C{\equiv}C}$ moieties of **6c** stabilise the mixed-valent forms $\mathbf{6c}^{3-6+}$ by additional repulsive electrostatic interactions.

For a further investigation of the electronic properties of **6a–c** *in situ* spectroelectrochemical UV–Vis/NIR measurements have been carried out to prove, if the interactions between the $\mathrm{Fc/Fc^+}$ groups are solely caused by electrostatic contributions or if an intramolecular electron transfer between the redox-active ferrocenyl moieties *via* the carbon-rich connectivities occurs.

Spectroelectrochemistry

The spectroelectrochemical studies were performed in an OTTLE (= Optically Transparent Thin-Layer Electrochemistry) cell[32] and the potential was increased stepwisely (step heights: 15 mV, 25 mV, 50 mV or 100 mV) from −200 to 1000 mV *vs.* Ag/AgCl. Dichloromethane solutions containing **6a**, **6b** or **6c** (0.001 mol L^{-1}) and $[^n\mathrm{Bu_4N}][\mathrm{B(C_6F_5)_4}]$ (0.1 mol L^{-1}) as electrolyte were used at 25 °C. Starting from neutral **6a–c**, the stepwise increase of the potential allows the *in situ* generation of cationic $\mathbf{6a\text{–}c}^{n+}$ (n = 1–4 (**6a**), n = 2 and n = 3 are formed at the same potential; 1–5 (**6b**); 1–6 (**6c**)) (Fig. 7, SI5 and SI6‡).

For neutral **6a,b**, as expected, no absorptions in the NIR region (1000–3000 nm) were observed. Upon subsequent oxidation steadily increasing absorptions with low extinctions (ε_{max} = 50–270 L mol^{-1} cm^{-1}) at 1270 nm ($\mathbf{6a}^{n+}$, n = 1–4) and 1300 nm ($\mathbf{6b}^{n+}$, n = 1–5) were found (Fig. SI5 and SI6‡). These absorptions can be assigned to LMCT (=*L*igand-to-*M*etal *C*harge *T*ransfer) transitions.[33] In the UV-Vis region (250–750 nm), excitations including the π–π* transitions of the benzene core as well as the d–d transitions of the Fc substituents could be detected.[34] Since no IVCT (=*I*nter-*V*alence *C*harge *T*ransfer) absorptions were observed, mainly electrostatic interactions (ΔE_e) are responsible for the observed redox splittings between the equally charged redox centres in $\mathbf{6a,b}^{n+}$ (**6a**, n = 2–4; **6b**, n = 2–5). Therefore, in **6a,b** any oxidation state can be classified as class I system according to Robin and Day.[35]

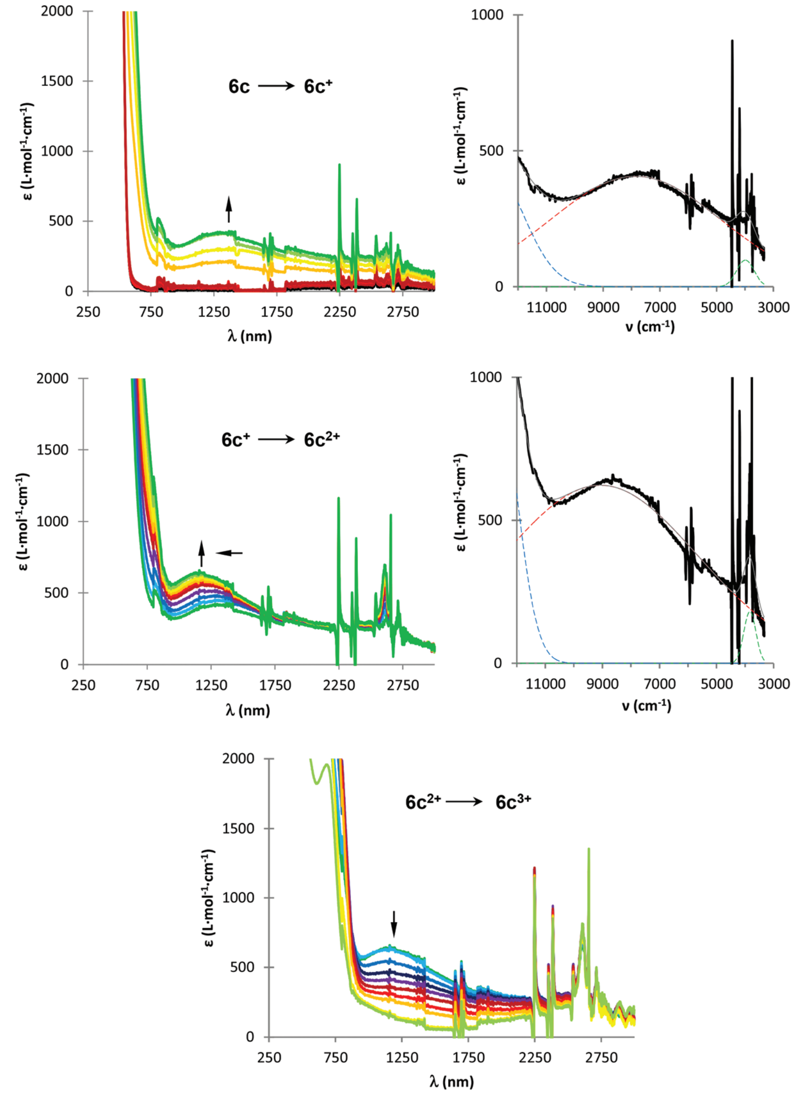

Fig. 7 Left: UV-Vis/NIR spectra of **6c** at rising potentials *vs.* Ag/AgCl: left −200 to 245 mV (left top), 245 to 400 mV (left middle), 400 to 1000 mV (bottom). Right: Deconvolution of the NIR absorptions at 245 mV (top) and 400 mV (middle) of *in situ* generated $\mathbf{6c}^{+}$ and $\mathbf{6c}^{2+}$ using three Gaussian-shaped graphs. Measurement conditions: 25 °C, dichloromethane, 0.1 mol L^{-1} [$^{n}Bu_4N$][$B(C_6F_5)_4$] as supporting electrolyte.

However, upon oxidation of **6c**, a weak and broad excitation in the NIR region (Fig. 7) was observed of which the band of the dicationic species is hypso- and hyperchromically shifted compared with $\mathbf{6c}^{+}$. The physical parameters have been determined by deconvolution of the experimental spectra using three Gaussian-shaped functions (Fig. 7) ($\mathbf{6c}^{+}$, ν_{max} = 7860 cm^{-1}, $\Delta\nu_{1/2}$ = 7070 cm^{-1}, ε_{max} = 405 L mol^{-1} cm^{-1}; $\mathbf{6c}^{2+}$, ν_{max} = 9070 cm^{-1}, $\Delta\nu_{1/2}$ = 8010 cm^{-1}, ε_{max} = 620 L mol^{-1} cm^{-1}). Due to the low absorption in the NIR region detected for $\mathbf{6c}^{+/2+}$, the compounds can be classified as weakly coupled class II systems according to Robin and Day.[35] On further oxidation of $\mathbf{6c}^{2+}$ to $\mathbf{6c}^{3+}$ (400 to 1000 mV) this excitation disappeared. The spectroelectrochemical behaviour of **6c** is similar to that of 1,3,5-$Fc_3C_6H_3$ and 2,4,6-$Fc_3C_5H_2N$ (1,3,5-$Fc_3C_6H_3^{+}$, ν_{max} = 6970 cm^{-1}, $\Delta\nu_{1/2}$ = 6240 cm^{-1}, ε_{max} = 35 L mol^{-1} cm^{-1}; 1,3,5-$Fc_3C_6H_3^{2+}$, ν_{max} = 6590 cm^{-1}, $\Delta\nu_{1/2}$ = 6220 cm^{-1}, ε_{max} = 105 L mol^{-1} cm^{-1} | 2,4,6-$Fc_3C_5H_2N^{+}$, ν_{max} = 6010 cm^{-1}, $\Delta\nu_{1/2}$ = 7515 cm^{-1}, ε_{max} = 30 L mol^{-1} cm^{-1}; 2,4,6-$Fc_3C_5H_2N^{2+}$, ν_{max} = 6290 cm^{-1}, $\Delta\nu_{1/2}$ = 7550 cm^{-1}, ε_{max} = 65 L mol^{-1} cm^{-1}).[1c] However, upon consecutive oxidation of 1,3,5-$Fc_3C_6H_3$ a bathochromic shift of the IVCT absorption was observed, while the IVCT transition of 2,4,6-$Fc_3C_5H_2N$ shifts hypsochromically, when oxidation from the mono- to the dicationic species takes place. This indicates that an increasing electron poorness of the aromatic core, caused by the nitrogen atom[1c] or the electron-withdrawing FcC≡C groups in **6c**, is responsible for the shift of the IVCT bands towards higher energy, when the mixed-valent Fe(II)/Fe(II)/Fe(III) species is oxidised to the Fe(II)/Fe(III)/Fe(III) system.

Besides the electronic interaction pathway along the *meta*-substituted directly bonded ferrocenyl units, an interaction between *ortho*-substituted Fc and FcC≡C moieties seems possible. In this respect, 1-FcC≡C-2-FcC_6H_4 (**9**) has been investigated by *in situ* UV-Vis/NIR spectroscopy. In contrast to the

UV-Vis/NIR spectrum of $\mathbf{6c}^{n+}$ (n = 1, 2) mixed-valent $\mathbf{9}^{+}$ shows no IVCT but a LMCT absorption at 760 cm^{-1} (Fig. SI9‡), indicating no electronic interactions between the Fe(II)/Fe(III) centres of the FcC≡C and Fc units. This observation confirms that the charge transfer in $\mathbf{6c}^{n+}$ (n = 1, 2) occurs solely between the directly bonded Fc/Fc^{+} termini.

The electron poor character of the benzene core of **6b**, caused by the electron-withdrawing effect of the chlorine in position 1, is not capable of facilitating the charge transfer between Fc/Fc^{+} in 3,5-positions.

Conclusion

A series of (multi)ferrocenyl-substituted benzenes such as 1,3,5-Cl_3-2-(FcC≡C)-4,6-I_2-C_6 (**4a**), 1,3,5-Cl_3-2,4-$(FcC≡C)_2$-6-I-C_6 (**4b**), 1,3,5-Cl_3-2,4,6-$(FcC≡C)_3$-C_6 (**4c**), 1,3-Cl_2-5-Fc-2,4,6-$(FcC≡C)_3$-C_6 (**6a**), 1-Cl-3,5-Fc_2-2,4,6-$(FcC≡C)_3$-C_6 (**6b**) and 1,3,5-Fc_3-2,4,6-$(FcC≡C)_3$-C_6 (**6c**) (Fc = Fe(η^5-C_5H_4)(η^5-C_5H_5)) have been prepared using palladium-catalysed Sonogashira and Negishi *C*,*C* cross-coupling reactions of halogenated aromatics with ethynylferrocene and ferrocenyl zinc chloride, respectively. The concentration of the $[PdCl_2(PPh_3)_2]$ and the amount of FcC≡CH in the Sonogashira *C*,*C* cross-coupling plays a crucial role for the formation of **4c**. The structures of **4a**,**b** and **6a**, in the solid state were determined by single crystal X-ray diffraction analysis. Compound **4b** forms a dimeric structure in the solid state, caused by parallel displaced π–π interactions between the centroids of the two C_6 cores of this dimer.[22] For **6a** more complex T-shaped π–π interactions, which are of intra- as well as of intermolecular type, occur. The redox properties of **4a–c** and **6a–c** were studied by cyclic and square wave voltammetry. The ferrocenyl units within compounds **4a–c** are oxidised simultaneously. The partial negative charge of the electronegative chlorine atom in between the Fc^{+} moieties of $\mathbf{4c}^{n+}$ (n = 2, 3) compensates the repulsive electrostatic Fc^{+}–Fc^{+} interactions with attractive electrostatic Fc^{+}–$Cl^{\delta-}$ interactions, destabilising the mixed-valent oxidation states. The absence of these chlorine atoms in 1,3,5-tris(ethynylferrocenyl) benzene thus leads to the observation of three well-separated reversible redox events, when weakly coordination anions as supporting electrolytes are applied.[6b,c,23] A comparison of ferrocenyl benzene[29] and ethynylferrocenyl benzene[30] shows that most likely the directly bonded ferrocenyl units are oxidised at lower potential than the ethynylferrocenyl units in **6a–c**. The first three redox events in **6c** are resolved into one-electron waves as is typical for triferrocenyl benzenes, oxidised separately. Furthermore, the ferrocenium units of $\mathbf{6c}^{3+}$ add further repulsive electrostatic interactions leading to a separate oxidation of the FcC≡C units. This also explains the different behaviour of **6c**, showing six reversible Fc–based one-electron oxidations compared to Astruc's $(FcC≡C)_6C_6$ in which only three redox events have been observed using comparable measurement conditions.

In addition, *in situ* UV-Vis/NIR studies revealed IVCT excitations in the mixed-valent oxidation states of $\mathbf{6c}^{+}$ and $\mathbf{6c}^{2+}$ attributed to the Fe(II)/Fe(III) metal centres of the directly bonded ferrocenyl groups. Therefore, the mixed-valent species $\mathbf{6c}^{n+}$ (n = 1, 2) can be classified as weakly coupled class II systems according to Robin and Day.[35] The spectroscopic characteristics of $\mathbf{6c}^{n+}$ (n = 1, 2) resemble those of 1,3,5-$Fc_3C_6H_3$ and 2,4,6-$Fc_3C_5H_2N$[1c] demonstrating that the electron transfer occurs between the Fc/Fc^{+} groups, while the pathway through the *ortho*-substituted Fc^{+}/FcC≡C units is unsuited for electronic interactions. This was confirmed by *in situ* UV-Vis/NIR investigations of 1-ethynylferrocenyl-2-ferrocenyl benzene (**9**) showing no IVCT absorptions in the mixed-valent oxidation state. Class I systems **6a**,**b** showed only LMCT transitions during these measurements.

Experimental section

General conditions

All reactions were carried out under an atmosphere of argon using standard Schlenk techniques. Drying of *n*-hexane, diethyl ether and dichloromethane was performed with a MBraun MB SPS-800 system (double column solvent filtration, working pressure 0.5 bar). Tetrahydrofuran was purified by distillation from sodium/benzophenone ketyl, and methanol was purified by distillation from magnesium. Diisopropylamine was purified by distillation from calcium hydride.

Reagents

Periodic acid, potassium iodide, 1,3,5-trichlorobenzene (**1**), triphenylphosphane, copper(I)iodide, ^{t}BuLi (1.9 M solution in *n*-pentane), ferrocene, 1-bromo-2-iodo-benzene (**7**) and KO^{t}Bu were purchased from commercial suppliers and were used without further purification. FcC≡CH (**3**),[36] $[{}^{n}Bu_4N][B(C_6F_5)_4]$[24] and $[PdCl_2(PPh_3)_2]$[37] were prepared according to published procedures. The palladium pre-catalyst $[P({}^{t}C_4H_9)_2C(CH_3)_2CH_2Pd(\mu\text{-}Cl)]_2$ was synthesized according to Clark *et al.*[38]

Instruments

${}^{1}H$ NMR (500.3 MHz) and ${}^{13}C\{{}^{1}H\}$ NMR (125.8 MHz) spectra were recorded with a Bruker Avance III 500 spectrometer operating at 298 K in the Fourier transform mode. Chemical shifts are reported in δ units (parts per million) using undeuterated solvent residues as internal standard ($CDCl_3$: ${}^{1}H$ at 7.26 ppm and ${}^{13}C\{{}^{1}H\}$ at 77.16 ppm). Infrared spectra were recorded using a FT-Nicolet IR 200 equipment. The melting points of analytical pure samples (sealed off in nitrogen-purged capillaries) were determined with a Gallenkamp MFB 595 010 M melting point apparatus. Microanalyses were performed using a Thermo FLASHEA 1112 Series instrument. High-resolution mass spectra were performed with a micrOTOF QII Bruker Daltonite workstation.

Single crystal X-ray diffraction analysis

Data for **4a**,**b** and **6a** were collected with an Oxford Gemini S diffractometer using graphite-monochromatised Mo Kα radiation (λ = 0.71073 Å). The molecular structures were solved by direct methods using SHELXS-97[39] and refined by full-matrix least-squares procedures on F^2 using SHELXL-97.[40] All non-hydrogen atoms were refined anisotropically and a riding model was employed in the treatment of the hydrogen atom positions.

Electrochemistry

Measurements on 1.0 mmol L^{-1} solutions of the analytes in dry air free dichloromethane containing 0.1 mol L^{-1} of $[^nBu_4N][B(C_6F_5)_4]$ as supporting electrolyte were conducted under a blanket of purified argon at 25 °C utilising a Radiometer Voltalab PGZ 100 electrochemical workstation interfaced with a personal computer. A three electrode cell, which utilised a Pt auxiliary electrode, a glassy carbon working electrode (surface area 0.031 cm^2), and an Ag/Ag^+ (0.01 mol L^{-1} $AgNO_3$) reference electrode mounted on a luggin capillary was used. The working electrode was pretreated by polishing on a Buehler microcloth first with a 1 µm and then with a 1/4 µm diamond paste. The reference electrode was built from a silver wire inserted into a solution of 0.01 mol L^{-1} $[AgNO_3]$ and 0.1 mol L^{-1} $[^nBu_4N][B(C_6F_5)_4]$ in acetonitrile, in a luggin capillary with a vycor tip. This luggin capillary was inserted into a second luggin capillary with a vycor tip filled with a 0.1 mol L^{-1} dichloromethane solution of $[^nBu_4N][B(C_6F_5)_4]$.[24] Successive experiments under the same experimental conditions showed that all formal reduction and oxidation potentials were reproducible within ±5 mV. Experimentally potentials were referenced against an Ag/Ag^+ reference electrode but results are presented referenced against ferrocene[41] (FcH/FcH^+ couple = 220 mV *vs.* Ag/Ag^+, ΔE_p = 61 mV) as an internal standard as required by IUPAC.[25] When decamethylferrocene was used as an internal standard, the experimentally measured potential was converted into E *vs.* FcH/FcH^+ (under our conditions the Fc^*/Fc^{*+} couple was at −614 mV *vs.* FcH/FcH^+, ΔE_p = 60 mV).[42] Data were then manipulated on a Microsoft Excel worksheet to set the formal redox potentials of the FcH/FcH^+ couple to $E^{\circ\prime}$ = 0.000 V. The cyclic voltammograms were taken after typical two scans and are considered to be steady state cyclic voltammograms in which the signal pattern differs not from the initial sweep.

Spectroelectrochemistry

Spectroelectrochemical UV-Vis/NIR measurements of 0.1 (**6c**) and 2.0 mmol L^{-1} solutions (**6a,b**) in dry dichloromethane containing 0.1 mol L^{-1} of $[^nBu_4N][B(C_6F_5)_4]$ as the supporting electrolyte were performed in an OTTLE (= optically transparent thin-layer electrochemistry, quartz windows for UV/Vis-NIR)[32] cell with a Varian Cary 5000 spectrophotometer (UV-Vis/NIR) at 25 °C. Between the spectroscopic measurements the applied potentials have been increased step-wisely using step heights of 15, 25, 50 or 100 mV. At the end of the measurements the analyte was reduced at −500 mV for 15 min and an additional spectrum was recorded to prove the reversibility of the oxidations.

Synthesis of 1,3,5-trichloro-2,4,6-triiodo-benzene (2)

The preparation of compound **2** was carried out using a modified procedure from the literature.[14] To 500 mL concentrated H_2SO_4 periodic acid (30.15 g; 132.3 mmol) was slowly added in small portions (5 g) at ambient temperature. For a complete dissolution of the periodic acid the reaction mixture was stirred vigorously. After adding KI (65.86 g; 411.6 mmol) at 0 °C in small portions (10 g) over 1 h, the resulting deep purple solution was treated with 1,3,5-trichlorobenzene (**1**) (7.00 g; 38.6 mmol) in three portions (2.33 g) over 25 min at 0 °C. The reaction mixture was allowed to warm to ambient temperature and stirred for 96 h. The mixture was poured onto ice (exothermic reaction!) and the precipitate was filtered and washed with H_2O until neutralisation and then washed with methanol (200 mL). The colorless residue was recrystallised from hot tetrahydrofuran affording colorless needle-shaped crystals. Yield: 18.12 g (32.39 mmol, 84% based on 1,3,5-trichlorobenzene (**1**)); colorless, crystalline solid, soluble in tetrahydrofuran. Anal. calcd for $C_6Cl_3I_3$ (559.14 g mol^{-1}) [%]: C, 12.89; found: C, 12.98. Mp.: 283 °C. $^{13}C\{^1H\}$ NMR [$CDCl_3$, ppm] δ: 98.00 (C–I), 145.78 (C–Cl). IR data [KBr, cm^{-1}] ν: 911 (m, ν_{C-I}), 1068 (m, ν_{C-Cl}).

General procedure – synthesis of 4a,b

In a Schlenk flask, 50 mL of degassed diisopropylamine, 6.00 mol% of CuI (65.3 mg, 0.34 mmol) and 0.50 mol% of $[PdCl_2(PPh_3)_2]$ (20 mg, 0.03 mmol) were added and the solution was stirred for 5 min. The reaction mixture was treated with 1.00 g (1.79 mmol) of **2**, 3.2 eq. of ethynylferrocene (**3**) (1.20 g, 5.7 mmol) and 6.00 mol% of PPh_3 (90.0 mg, 0.34 mmol) and was then heated to reflux for 24 h, whereby the crimson solution turned orange. After cooling it to room temperature and evaporation of all volatiles, the orange residue was worked-up by column chromatography (column size: 3 × 10 cm, alumina, *n*-hexane). As eluent a *n*-hexane–diethyl ether mixture of ratio 20 : 1 (v/v) was used. The 1st fraction contained ethynylferrocene (**3**), while from the 2nd fraction **4a** and from the 3rd fraction **4b** could be isolated. All volatiles were removed under reduced pressure.

1,3,5-Trichloro-2-ethynylferrocenyl-4,6-diiodo-benzene (4a)

Yield: 40 mg (0.062 mmol, 4% based on **2**), orange solid, soluble in dichloromethane. Anal. calcd for $C_{18}H_9FeCl_3I_2\cdot0.08C_6H_{14}$ (648.17 g mol^{-1}) [%]: C, 34.24; H, 1.57; found: C, 34.24; H, 1.39. Mp.: 210 °C. ^1H NMR [$CDCl_3$, ppm] δ: 4.27 (s, 5 H, C_5H_5), 4.32 (pt, J_{HH} = 1.90 Hz, 2 H, C_5H_4), 4.58 (pt, J_{HH} = 1.90 Hz, 2 H, C_5H_4). $^{13}C\{^1H\}$ NMR [$CDCl_3$, ppm] δ: 63.27 ($FcC{\equiv}CC_6$), 69.84 (C_5H_4), 70.42 (C_5H_5), 72.10 (C_5H_4), 81.38 (C_i-C_5H_4), 100.59 (C–I), 101.58 ($Fc\mathbf{C}{\equiv}CC_6$), 121.90 ($FcC{\equiv}\mathbf{C}C_6$), 142.09 (C–Cl, C-1/3), 143.63 (C–Cl, C-5). IR data [KBr, cm^{-1}] ν: 826 (s, $\delta_{o.o.p.\ =C-H}$), 1023 (m, $\nu_{=C-Cl}$), 1315 (s, ν_{C-H}), 1526 (w, $\nu_{C=C}$), 2219 (s, $\nu_{C\equiv C}$), 3075 (w, $\nu_{=C-H}$). HR-ESI-MS [m/z]: calcd for $C_{18}H_9FeCl_3I_2$: 639.7154, found: 639.7204 [M^+].

Crystal data for 4a

Single crystals of **4a** were obtained by evaporation of a dichloromethane solution containing **4a** at 25 °C. $C_{18}H_9FeCl_3I_2$, M_r = 641.25 g mol^{-1}, crystal dimension 0.38 × 0.2 × 0.2 mm, triclinic, $P\bar{1}$, λ = 0.71073 Å, a = 7.4387(5) Å, b = 10.1811(8) Å, c = 13.7230(8) Å, α = 69.747(6)°, β = 74.437(6)°, γ = 72.227(7)°, V = 912.99(11) Å^3, Z = 2, ρ_{calcd} = 2.333 g cm^{-3}, μ = 4.643 mm^{-1}, T = 110 K, Θ range = 3.03–26.00°, reflections collected 6949, independent 3562, R_1 = 0.0243, wR_2 = 0.0497 [$I \geq 2\sigma(I)$].

1,3,5-Trichloro-2,4-bis(ethynylferrocenyl)-6-iodo-benzene (4b)

Yield: 0.333 g (0.46 mmol, 26% based on **2**), red-orange solid, soluble in dichloromethane. Anal. calcd for $C_{30}H_{18}Fe_2Cl_3I$ (723.42 g mol^{-1}) [%]: C, 49.81; H, 2.51; found: C, 49.68; H, 2.59. Mp.: 230 °C (decomp.). ^{1}H NMR [$CDCl_3$, ppm] δ: 4.28 (s, 10 H, C_5H_5), 4.32 (pt, J_{HH} = 1.90 Hz, 4 H, C_5H_4), 4.60 (pt, J_{HH} = 1.90 Hz, 4 H, C_5H_4). $^{13}C\{^1H\}$ NMR [$CDCl_3$, ppm] δ: 63.68 (FcC≡**C**C_6), 69.80 (C_5H_4), 70.48 (C_5H_5), 72.11 (C_5H_4), 80.41 (C_i-C_5H_4), 101.40 (Fc**C**≡CC_6), 102.35 (C–I), 122.93 (FcC≡C**C**$_6$), 138.30 (C–Cl, C-3), 140.32 (C–Cl, C-1/5). IR data [KBr, cm^{-1}] ν: 818 (s, $\delta_{o.o.p.\ =C-H}$), 1002, 1024 (m, $\nu_{=C-Cl}$), 1346 (s, ν_{C-H}), 1540 (w, $\nu_{C=C}$), 2209 (s, $\nu_{C\equiv C}$), 3097 (w, $\nu_{=C-H}$). HR-ESI-MS [m/z]: calcd for $C_{30}H_{18}Fe_2Cl_3I$: 721.8215, found: 721.8275 [M$^+$].

Crystal data for 4b

Single crystals of **4b** were obtained by diffusion of methanol into a dichloromethane solution containing **4b** at 25 °C. $C_{60}H_{36}Fe_4Cl_6I_2$, M_r = 1446.79 g mol^{-1}, crystal dimension 0.2 × 0.05 × 0.05 mm, monoclinic, $C2/c$, λ = 0.71073 Å, a = 27.984(2) Å, b = 9.9891(4) Å, c = 20.7362(17) Å, β = 119.178(10)°, V = 5061.0(7) Å^3, Z = 4, ρ_{calcd} = 1.899 g cm^{-3}, μ = 2.703 mm^{-1}, T = 110 K, Θ range = 2.978–24.998°, reflections collected 12 898, independent 4411, R_1 = 0.1063, wR_2 = 0.2768 [$I \geq 2\sigma(I)$].

Synthesis of 1,3,5-trichloro-2,4,6-tris(ethynylferrocenyl) benzene (4c)

In a Schlenk flask, 50 mL of degassed diisopropylamine, 6.00 mol% of CuI (81.7 mg, 0.43 mmol) and 1.00 mol% of [$PdCl_2(PPh_3)_2$] (50 mg, 0.07 mmol) were added and the solution was stirred for 5 min. The reaction mixture was treated with 1.00 g (1.79 mmol) of 1,3,5-trichloro-2,4,6-triiodobenzene, 4 eq. of ethynylferrocene (**3**) (1.50 g, 7.15 mmol) and 6.00 mol% of PPh_3 (113.0 mg, 0.43 mmol) and was afterwards heated to reflux for 24 h whereby the crimson solution turned into an orange suspension. After cooling it to room temperature and evaporation of all volatiles, the orange residue was worked-up by Soxhlet extraction with diethyl ether (20 h) to remove the appropriate ammonium salt. The obtained orange precipitate was filtered off and washed with cold diethyl ether (2 × 10 mL). The product was dried in oil pump vacuum. Yield: 1.34 g (1.66 mmol, 93% based on 1,3,5-trichloro-2,4,6-triiodobenzene); orange solid, soluble in dichloromethane. Anal. calcd for $C_{42}H_{27}Fe_3Cl_3$ (805.56 g mol^{-1}) [%]: C, 62.62; H, 3.38; found: C, 62.23; H, 3.61. Mp.: 185 °C (decomp.). ^{1}H NMR [$CDCl_3$, ppm] δ: 4.30 (s, 15 H, C_5H_5), 4.32 (pt, J_{HH} = 1.90 Hz, 6 H, C_5H_4), 4.61 (pt, J_{HH} = 1.90 Hz, 6 H, C_5H_4). $^{13}C\{^1H\}$ NMR [$CDCl_3$, ppm] δ: 63.91 (FcC≡**C**C_6), 69.65 (C_5H_4, FcC≡C), 70.43 (C_5H_5, FcC≡C), 72.05 (C_5H_4, FcC≡C), 79.60 (C_i-C_5H_4, FcC≡C), 101.04 (Fc**C**≡CC_6), 123.55 (FcC≡C**C**$_6$), 136.76 (C–Cl). IR data [KBr, cm^{-1}] ν: 824 (s, $\delta_{o.o.p.\ =C-H}$), 1025 (m, $\nu_{=C-Cl}$), 1359, 1383 (s, ν_{C-H}), 1532 (w, $\nu_{C=C}$), 2209 (s, $\nu_{C\equiv C}$), 3088 (w, $\nu_{=C-H}$). HR-ESI-MS [m/z]: calcd for $C_{42}H_{27}Fe_3Cl_3$: 803.9226, found: 803.9222 [M$^+$].

General procedure – synthesis of 6a–c

Ferrocene (1.795 g, 9.7 mmol) and KO^{t}Bu (0.125 eq., 0.135 g, 1.2 mmol) were dissolved in 60 mL of tetrahydrofuran and the solution was cooled to −80 °C. ^{t}Butyllithium (2 eq., 1.9 M in n-pentane, 10.15 mL) was added dropwise *via* a syringe and the solution was stirred for 1 h. Then [$ZnCl_2$·2thf] (1 eq., 2.70 g, 9.7 mmol) was added in a single portion. The reaction mixture was stirred for additional 30 min at 0 °C. Afterwards, 0.25 mol % of [$Pd(CH_2C(CH_3)_2P(^tC_4H_9)_2)(\mu\text{-}Cl)]_2$ (0.025 g, 0.004 mmol) and 1/6 eq. of **4c** (1.295 g, 1.61 mmol) were added in a single portion and the reaction solution was stirred at 80 °C for 60 h. The crude product was purified by column chromatography (column size: 1.5 × 10 cm, alumina, n-hexane). As eluent a n-hexane–diethyl ether mixture of ratio 30 : 1 (v/v) was used. The first fraction contained ferrocene and unknown compounds, while thereafter 1,3-dichloro-5-ferrocenyl-2,4,6-tris(ethynylferrocenyl) benzene (**6a**) and 1-chloro-3,5-diferrocenyl-2,4,6-tris(ethynylferrocenyl) benzene (**6b**) were eluted. Pure **6c** could be isolated using dichloromethane as eluent. All volatiles were removed under reduced pressure.

1,3-Dichloro-5-ferrocenyl-2,4,6-tris(ethynylferrocenyl) benzene (6a)

Yield: 0.046 g (0.05 mmol, 3% based on **4c**), orange solid, soluble in dichloromethane. Anal. calcd for $C_{52}H_{36}Fe_4Cl_2$ (955.13 g mol^{-1}) [%]: C, 65.39; H, 3.80; found: C, 65.72; H, 4.36. Mp.: 209 °C. ^{1}H NMR [$CDCl_3$, ppm] δ: 4.23 (s, 5 H, C_5H_5, 2-FcC≡C), 4.30 (s, 10 H, C_5H_5, 4,6-FcC≡C), 4.32 (pt, J_{HH} = 1.90 Hz, 2 H, C_5H_4, 2-FcC≡C), 4.32 (s, 5 H, C_5H_5, Fc), 4.33 (pt, J_{HH} = 1.90 Hz, 4 H, C_5H_4, 4,6-FcC≡C), 4.48 (pt, J_{HH} = 1.90 Hz, 2 H, C_5H_4, Fc), 4.61 (pt, J_{HH} = 1.90 Hz, 4 H, C_5H_4, 4,6-FcC≡C), 4.63 (pt, J_{HH} = 1.90 Hz, 2 H, C_5H_4, 2-FcC≡C), 5.41 (pt, J_{HH} = 1.90 Hz, 2 H, C_5H_4, Fc). $^{13}C\{^1H\}$ NMR [$CDCl_3$, ppm] δ: 64.51 (2-FcC≡**C**C_6), 65.30 (4,6-FcC≡**C**C_6), 68.47 (C_5H_4, 5-Fc), 69.41 (C_5H_4, 4,6-FcC≡C), 69.49 (C_5H_4, 2-FcC≡C), 70.20 (C_5H_5, 4,6-FcC≡C), 70.37 (C_5H_5, 2-FcC≡C), 70.40 (C_5H_5, 5-Fc), 71.45 (C_5H_4, 4,6-FcC≡C), 71.72 (C_5H_4, 5-Fc), 71.98 (C_5H_4, 2-FcC≡C), 80.71 (C_i-C_5H_4, 2-FcC≡C), 82.65 (C_i-C_5H_4, 5-Fc), 83.61 (C_i-C_5H_4, 4,6-FcC≡C), 99.66 (2-Fc**C**≡CC_6), 101.21 (4,6-Fc**C**≡CC_6), 122.04 (4,6-FcC≡C**C**$_6$), 122.22 (2-FcC≡C**C**$_6$), 138.13 (C–Cl, C-1,3), 143.27 (5-Fc-**C**$_6$). IR data [KBr, cm^{-1}] ν: 818 (s, $\delta_{o.o.p.\ =C-H}$), 1000 (m, $\nu_{=C-Cl}$), 1360 (m, ν_{C-H}), 1531 (w, $\nu_{C=C}$), 2213 (s, $\nu_{C\equiv C}$), 3089 (w, $\nu_{=C-H}$). HR-ESI-MS [m/z]: calcd for $C_{52}H_{36}Fe_4Cl_2$: 953.9593, found: 953.9537 [M$^+$].

Crystal data for 6a

Single crystals of **6a** were obtained by evaporation of a dichloromethane solution containing **6a** at 25 °C. $C_{52}H_{36}Fe_4Cl_2$,

M_r = 955.11 g mol^{-1}, crystal dimension 0.4 × 0.3 × 0.02 mm, orthorhombic, *Pccn*, λ = 0.71073 Å, a = 12.8015(6) Å, b = 32.736(3) Å, c = 18.6516(10) Å, $\alpha = \beta = \gamma$ = 90°, V = 7816.4(9) Å^3, Z = 8, ρ_{calcd} = 1.623 g cm^{-3}, μ = 1.631 mm^{-1}, T = 110 K, Θ range = 2.873–25.00°, reflections collected 41 618, independent 6835, R_1 = 0.1591, wR_2 = 0.3167 [$I \geq 2\sigma(I)$].

1-Chloro-3,5-diferrocenyl-2,4,6-tris(ethynylferrocenyl) benzene (6b)

Yield: 0.622 g (0.56 mmol, 35% based on **4c**), red solid, soluble in dichloromethane. Anal. calcd for $C_{62}H_{45}Fe_5Cl$ (1104.70 g mol^{-1}) [%]: C, 67.41; H, 4.11; found: C, 67.25; H, 4.47. Mp.: 148 °C. ^{1}H NMR [$CDCl_3$, ppm] δ: 4.17 (s, 5 H, C_5H_5, 4-FcC≡C), 4.26 (s, 10 H, C_5H_5, 2,6-FcC≡C), 4.27 (pt, J_{HH} = 1.90 Hz, 2 H, C_5H_4, 4-FcC≡C), 4.32 (s, 10 H, C_5H_5, 3,5-Fc), 4.33 (pt, J_{HH} = 1.90 Hz, 4 H, C_5H_4, 2,6-FcC≡C), 4.46 (pt, J_{HH} = 1.90 Hz, 4 H, C_5H_4, 3,5-Fc), 4.48 (pt, J_{HH} = 1.90 Hz, 2 H, C_5H_4, 4-FcC≡C), 4.64 (pt, J_{HH} = 1.90 Hz, 4 H, C_5H_4, 2,6-FcC≡C), 5.32 (pt, J_{HH} = 1.90 Hz, 4 H, C_5H_4, 3,5-Fc). ^{13}C{^{1}H} NMR [$CDCl_3$, ppm] δ: 65.96 (2,6-FcC≡**C**C$_6$), 66.45 (4-FcC≡**C**C$_6$), 67.80 (C_5H_4, 3,5-Fc), 69.04 (C_5H_4, 4-FcC≡C), 69.30 (C_5H_4, 2,6-FcC≡C), 70.01 (C_5H_5, 4-FcC≡C), 70.19 (C_5H_5, 3,5-Fc), 70.30 (C_5H_5, 2,6-FcC≡C), 70.70 (C_5H_4, 4-FcC≡C), 71.42 (C_5H_4, 2,6-FcC≡C), 72.26 (C_5H_4, 3,5-Fc), 83.76 (C_i-C_5H_4, 2,6-FcC≡C), 84.44 (C_i-C_5H_4, 4-FcC≡C), 88.01 (C_i-C_5H_4, 3,5-Fc), 99.57 (4-Fc**C**≡CC$_6$), 101.03 (2,6-Fc**C**≡CC$_6$), 121.59 (2,6-FcC≡C**C**$_6$), 121.92 (4-FcC≡C**C**$_6$), 139.36 (C–Cl, C-1), 143.05 (3,5-Fc-**C**$_6$). IR data [KBr, cm^{-1}] ν: 818 (s, $\delta_{o.o.p.\ =C-H}$), 1000 (m, $\nu_{=C-Cl}$), 1386 (m, ν_{C-H}), 1538 (w, $\nu_{C=C}$), 2205 (s, $\nu_{C\equiv C}$), 3084 (w, $\nu_{=C-H}$). HR-ESI-MS [m/z]: calcd for $C_{62}H_{45}Fe_5Cl$: 1103.9962, found: 1103.9947 [M$^+$].

2,4,6-Triferrocenyl-1,3,5-tris(ethynylferrocenyl) benzene (6c)

Yield: 0.230 g (0.18 mmol, 11% based on **4c**), orange solid, soluble in dichloromethane. Anal. calcd for $C_{72}H_{54}Fe_6$ (1254.27 g mol^{-1}) [%]: C, 68.95; H, 4.34; found: C, 69.01; H, 4.51. Mp.: 240 °C (decomp.). ^{1}H NMR [$CDCl_3$, ppm] δ: 4.19 (s, 15 H, C_5H_5, Fc), 4.29 (pt, J_{HH} = 1.90 Hz, 6 H, C_5H_4, FcC≡C), 4.31 (s, 15 H, C_5H_5, FcC≡C), 4.47 (pt, J_{HH} = 1.90 Hz, 6 H, C_5H_4, Fc), 4.54 (pt, J_{HH} = 1.90 Hz, 6 H, C_5H_4, FcC≡C), 5.24 (pt, J_{HH} = 1.90 Hz, 6 H, C_5H_4, Fc). ^{13}C{^{1}H} NMR [$CDCl_3$, ppm] δ: 67.09 (FcC≡**C**C$_6$), 67.25 (C_5H_4, Fc), 69.00 (C_5H_4, FcC≡C), 70.05 (C_5H_5, Fc), 70.21 (C_5H_5, FcC≡C), 70.67 (C_5H_4, FcC≡C), 72.80 (C_5H_4, Fc), 85.05 (C_i–C_5H_4, FcC≡C), 88.46 (C_i–C_5H_4, Fc), 100.62 (Fc**C**≡CC$_6$), 122.46 (FcC≡C**C**$_6$), 142.42 (Fc–**C**$_6$). IR data [KBr, cm^{-1}] ν: 818 (s, $\delta_{o.o.p.\ =C-H}$), 1106 (s, ν_{C-C}), 1383, 1411 (w, ν_{C-H}), 2210 (s, $\nu_{C\equiv C}$), 3094 (w, $\nu_{=C-H}$). HR-ESI-MS [m/z]: calcd for $C_{72}H_{54}Fe_6$: 1254.0331, found: 1254.0325 [M$^+$].

Acknowledgements

We are grateful to the Fonds der Chemischen Industrie (FCI) for generous financial support. Dipl.-Chem. M. Korb thanks the FCI for a Ph.D. fellowship. We thank Dipl.-Chem. J. M. Speck for fruitful discussions.

Notes and references

1 (*a*) P. Jutzi and B. Kleinebekel, *J. Organomet. Chem.*, 1997, **545–546**, 573–576; (*b*) M. Iyoda, T. Kondo, T. Okabe, H. Matsuyama, S. Sasaki and Y. Kuwatani, *Chem. Lett.*, 1997, **35**, 35–36; (*c*) U. Pfaff, A. Hildebrandt, D. Schaarschmidt, T. Hahn, S. Liebing, J. Kortus and H. Lang, *Organometallics*, 2012, **31**, 6761–6771; (*d*) K. Kaleta, A. Hildebrandt, F. Strehler, P. Arndt, H. Jiao, A. Spannenberg, H. Lang and U. Rosenthal, *Angew. Chem., Int. Ed.*, 2011, **50**, 11248–11252; (*e*) K. Kaleta, F. Strehler, A. Hildebrandt, T. Beweries, P. Arndt, T. Rüffer, A. Spannenberg, H. Lang and U. Rosenthal, *Chem. – Eur. J.*, 2012, **18**, 12672–12680; (*f*) R. Maragani and R. Misra, *Tetrahedron Lett.*, 2013, **54**, 5399–5402.

2 (*a*) C. Levanda, K. Bechgaard and D. O. Cowan, *J. Org. Chem.*, 1976, **41**, 2700–2704; (*b*) N. G. Connelly and W. E. Geiger, *Chem. Rev.*, 1996, **96**, 877–910; (*c*) K. Heinze and H. Lang, *Organometallics*, 2013, **32**, 5623–5625; (*d*) C. M. Casado, I. Cuadrado, M. Moran, B. Alonso, B. Garcia, B. Gonzales and J. Losada, *Coord. Chem. Rev.*, 1999, **185–186**, 53–79; (*e*) S. H. Hwang, C. D. Shreiner, C. N. Moorefield and G. N. Newkome, *New J. Chem.*, 2007, **31**, 1027–1038; (*f*) D. Astruc, C. Ornelas and J. Ruiz, *Acc. Chem. Res.*, 2008, **41**, 841–856.

3 (*a*) B. Helms and J. M. J. Fréchet, *Adv. Synth. Catal.*, 2006, **348**, 1125–1148; (*b*) D. Astruc, *Organometallic Chemistry and Catalysis*, Springer, Heidelberg, 2007, ch. 5, 16, and 19; (*c*) B. D. Chandler and J. D. Gilbertson, *Top. Organomet. Chem.*, 2006, **20**, 97–120.

4 (*a*) D. Astruc, *Electron Transfer and Radical Processes in Transition Metal Chemistry*, VCH, New York, 1995; (*b*) *Electron and Proton Transfer in Chemistry and Biology*, ed. A. Müller, H. Ratajczak, W. Junge and E. Dieman, Elsevier, New York, 1992; (*c*) H. B. Gray and J. R. Winkler, *Annu. Rev. Biochem.*, 1996, **65**, 537–561; (*d*) H. B. Gray and J. R. Winkler, *Biochim. Biophys. Acta, Bioenerg.*, 2010, **1797**, 1563–1572.

5 (*a*) S. Brydges, L. E. Harrington and M. J. McGlinchey, *Coord. Chem. Rev.*, 2002, **233–234**, 75–105; (*b*) S. C. Jones, S. Barlow and D. O'Hare, *Chem. – Eur. J.*, 2005, **11**, 4473–4481; (*c*) S. Barlow and S. D. O'Hare, *Chem. Rev.*, 1997, **97**, 637–670; (*d*) I. M. Bruce, *Coord. Chem. Rev.*, 1997, **166**, 91–119; (*e*) M. Ratner and J. Jortner, *Molecular Electronics*, Blackwell Science, Malden, MA, 1997; (*f*) R. L. Carroll and Ch. B. Gorman, *Angew. Chem.*, 2002, **114**, 4556–4579, (*Angew. Chem. Int. Ed.*, 2002, **41**, 4378–4400); (*g*) N. Robertson and C. A. McGowan, *Chem. Soc. Rev.*, 2003, **32**, 96–103.

6 (*a*) H. Fink, N. J. Long, A. J. Martin, G. Opromolla, A. J. P. White, D. J. Williams and P. Zanello, *Organometallics*, 1997, **16**, 2646–2650; (*b*) A. K. Diallo, J.-C. Daran, F. Varret, J. Ruiz and D. Astruc, *Angew. Chem., Int. Ed.*, 2009, **48**, 3141–3145; (*c*) A. K. Diallo, C. Absalon, J. Ruiz and D. Astruc, *J. Am. Chem. Soc.*, 2011, **133**, 629–641; (*d*) A. Trujillo, R. Veillard, G. Argouarch, T. Roisnel, A. Singh, I. Ledoux and F. Paul, *Dalton Trans.*, 2012, **41**,

7454–7456; (*e*) Y. Wang, A. K. Diallo, C. Ornelas, J. Ruiz and D. Astruc, *Inorg. Chem.*, 2012, **51**, 119–127.

7 (*a*) S. Dietrich, A. Nicolai and H. Lang, *J. Organomet. Chem.*, 2011, **696**, 739–747; (*b*) M. Lamač, J. Tauchman, S. Dietrich, S. Císařová, H. Lang and P. Štěpnička, *Appl. Organomet. Chem.*, 2010, **24**, 326–331.

8 S. Fiorentini, B. Floris, P. Galloni, F. Grepioni, M. Polito and P. Tagliatesta, *Eur. J. Org. Chem.*, 2006, 1726–1732.

9 Y. Yu, A. D. Bond, P. W. Leonard, U. J. Lorenz, T. V. Timofeeva, K. P. C. Vollhardt, G. D. Whitener and A. A. Yakovenko, *Chem. Commun.*, 2006, 2572–2574.

10 (*a*) A. Hildebrandt, T. Rüffer, E. Erasmus, J. C. Swarts and H. Lang, *Organometallics*, 2010, **29**, 4900–4905; (*b*) A. Hildebrandt and H. Lang, *Organometallics*, 2013, **32**, 5640–5653.

11 J. M. Speck, D. Schaarschmidt and H. Lang, *Organometallics*, 2012, **31**, 1975–1982.

12 J. Jiao, G. J. Long, L. Rebbouh, F. Grandjean, A. M. Beatty and T. P. Fehlner, *J. Am. Chem. Soc.*, 2005, **127**, 17819–17831.

13 Y. Yu, A. D. Bond, P. W. Leonard, K. P. C. Vollhardt and G. D. Whitener, *Angew. Chem., Int. Ed.*, 2006, **45**, 1794–1799.

14 (*a*) K. Kobayashi and N. Kobayashi, *J. Org. Chem.*, 2004, **69**, 2487–2497; (*b*) C. M. Reddy, M. T. Kirchner, R. C. Gundakaram, K. A. Padmanabhan and G. R. Desiraju, *Chem. – Eur. J.*, 2006, **12**, 2222–2234.

15 L. Skulski, *Molecules*, 2000, **5**, 1331–1371.

16 (*a*) K. Sonogashira, Y. Tohda and N. Hagihara, *Tetrahedron Lett.*, 1975, **16**, 4467–4470; (*b*) K. Sonogashira, *J. Organomet. Chem.*, 2002, **653**, 46–49.

17 (*a*) E. Negishi and F. Liu, in *Metal-Catalyzed Cross-Coupling Reactions*, ed. F. Diederich and P. J. Stang, Wiley-VCH, New York, 1997; (*b*) A. Carella, G. Rapenne and J.-P. Launay, *New J. Chem.*, 2005, **29**, 288–290.

18 G. Filipczyk, A. Hildebrandt, U. Pfaff, M. Korb, T. Rüffer and H. Lang, *Eur. J. Inorg. Chem.*, 2014, DOI: 10.1002/ejic.201402659.

19 H. Günther, *Angew. Chem., Int. Ed.*, 1972, **11**, 861–874.

20 H. Günzler and H. Böck, *IR-Spektroskopie*, VCH-Weinheim, zweite überarb. Aufl., 1983.

21 (*a*) J. Buddrus, *Grundlagen der Organischen Chemie*, De Gruyter, Berlin, 4th edn, 2011, pp. 368–369; (*b*) Please note that the six membered cycles of the main and the disordered part of molecule **4b** have been refined with an afix66 instruction for ideal C_6-rings and thus, the *C*,*C* bond lengths cannot be discussed.

22 This distance was calculated between the C_6-plane and the centroid of the transcripted C_6-cycle. The displaced C_6-planes obtain directly stacked atoms that are also in the range of π–π interactions (C28–C30_$1 and C30–C28_$1 (3.63(2); centroid-C29_$1 3.636(12) Å). Symmetry operation for generating equivalent atoms: $ = $-x$, $1 - y$, $-z$. For calculations of displaced π–π-interactions, see: M. O. Sinnokrot, E. F. Valeev and C. D. Sherrill, *J. Am. Chem. Soc.*, 2002, **124**, 10887–10893.

23 F. Barrière and W. E. Geiger, *J. Am. Chem. Soc.*, 2006, **128**, 3980–3989.

24 (*a*) U. Pfaff, A. Hildebrandt, D. Schaarschmidt, T. Rüffer, P. J. Low and H. Lang, *Organometallics*, 2013, **32**, 6106–6117; (*b*) R. J. LeSuer, C. Buttolph and W. E. Geiger, *Anal. Chem.*, 2004, **76**, 6395–6401; (*c*) H. J. Gericke, N. I. Barnard, E. Erasmus, J. C. Swarts, M. J. Cook and M. a. S. Aquino, *Inorg. Chim. Acta*, 2010, **363**, 2222–2232; (*d*) E. Fourie, J. C. Swarts, D. Lorcy and N. Bellec, *Inorg. Chem.*, 2010, **49**, 952–959; (*e*) J. C. Swarts, A. Nafady, J. H. Roudebush, S. Trupia and W. E. Geiger, *Inorg. Chem.*, 2009, **48**, 2156–2165; (*f*) D. Chong, J. Slote and W. E. Geiger, *J. Electroanal. Chem.*, 2009, **630**, 28–34; (*g*) V. N. Nemykin, G. T. Rohde, C. D. Barrett, R. G. Hadt, C. Bizzarri, P. Galloni, B. Floris, I. Nowik, R. H. Herber, A. G. Marrani, R. Zanoni and N. M. Loim, *J. Am. Chem. Soc.*, 2009, **131**, 14969–14978; (*h*) V. N. Nemykin, G. T. Rohde, C. D. Barrett, R. G. Hadt, J. R. Sabin, G. Reina, P. Galloni and B. Floris, *Inorg. Chem.*, 2010, **49**, 7497–7509; (*i*) A. Hildebrandt, D. Schaarschmidt and H. Lang, *Organometallics*, 2011, **30**, 556–563.

25 G. Gritzner and J. Kuta, *Pure Appl. Chem.*, 1984, **56**, 461–466.

26 A. Hildebrandt and H. Lang, *Dalton Trans.*, 2011, **40**, 11831–11837.

27 R. F. Winter, *Organometallics*, 2014, Article ASAP, DOI: 10.1021/om500029x.

28 F. Barrière, *Organometallics*, 2014, Article ASAP, DOI: 10.1021/om500248z.

29 M. C. P. Wang, Y. Li, N. Merbouh and H.-Z. Yu, *Electrochim. Acta*, 2008, **53**, 7720–7725.

30 T. Bobula, J. Hudlicky, P. Novak, R. Gyepes, I. Císařǒvá, P. Štěpnička and M. Kotora, *Eur. J. Inorg. Chem.*, 2008, 3911–3920.

31 D. E. Richardson and H. Taube, *Inorg. Chem.*, 1981, **20**, 1278–1285.

32 M. Krejčik, M. Daněk and F. Hartl, *J. Electroanal. Chem.*, 1991, **317**, 179–187.

33 A. Hildebrandt, T. Rüffer, E. Erasmus, J. C. Swarts and H. Lang, *Organometallics*, 2010, **29**, 4900–4905.

34 H. B. Gray, Y. S. Sohn and N. Hendrickson, *J. Am. Chem. Soc.*, 1971, **93**, 3603–3612.

35 M. B. Robin and P. Day, *Adv. Inorg. Chem. Radiochem.*, 1967, **10**, 247–422.

36 J. Polin and H. Schottenberger, *Org. Synth.*, 1996, **73**, 262–267.

37 N. Miyaura and A. Suzuki, *Org. Synth.*, 1990, **68**, 130–132.

38 H. C. Clark and A. B. Goel, *Inorg. Chim. Acta*, 1978, **31**, 441–442.

39 G. M. Sheldrick, *Acta Crystallogr., Sect. A: Fundam. Crystallogr.*, 1990, **46**, 467–473.

40 G. M. Sheldrick, *Program for Crystal Structure Refinement*, Universität Göttingen, Göttingen, Germany, 1997.

41 (*a*) I. Noviandri, K. N. Brown, D. S. Fleming, P. T. Gulyas, P. A. Lay, A. F. Masters and L. Phillips, *J. Phys. Chem. B*, 1999, **103**, 6713–6722; (*b*) J. Ruiz, M. C. Daniel and D. Astruc, *Can. J. Chem.*, 2006, **84**, 288–299.

42 A. Nafady and W. E. Geiger, *Organometallics*, 2008, **27**, 5624–5631.